
Supernet Training for Federated Image Classification under System Heterogeneity

Taehyeon Kim
 KAIST AI
 Seoul, South Korea
 potter32@kaist.ac.kr

Se-Young Yun
 KAIST AI
 Seoul, South Korea
 yunseyoung@gmail.com

Abstract

Efficient deployment of deep neural networks across many devices and resource constraints, especially on edge devices, is one of the most challenging problems in the presence of data-privacy preservation issues. Conventional approaches have evolved to either improve a single global model while keeping each local training data decentralized (i.e., data-heterogeneity) or to train a once-for-all network that supports diverse architectural settings to address heterogeneous systems equipped with different computational capabilities (i.e., model-heterogeneity). However, little research has considered both directions simultaneously. In this work, we propose a novel framework to consider both scenarios, namely Federation of Supernet Training (FedSup), where clients send and receive a supernet whereby it contains all possible architectures sampled from itself. It is inspired by how averaging parameters in the model aggregation stage of Federated Learning (FL) is similar to weight-sharing in supernet training. Specifically, in the FedSup framework, a weight-sharing approach widely used in the training single shot model is combined with the averaging of Federated Learning (FedAvg). Under our framework, we present an efficient algorithm (E-FedSup) by sending the sub-model to clients on the broadcast stage to reduce communication costs and training overhead. We demonstrate several strategies to enhance supernet training in the FL environment and conduct extensive empirical evaluations. The resulting framework is shown to pave the way for the robustness of both data- and model-heterogeneity on several standard benchmarks.

1 Introduction

Deep neural networks (DNN) have achieved remarkable empirical success in many machine learning applications. As a next evolution, there has been an increasing demand for training a model by using local data from mobile devices and the Internet of Things (IoT) because billions of local machines worldwide can bring more computational power and amounts of data than those of the center server machine [37; 10]. However, it is still challenging to deploy them efficiently on diverse hardware platforms whose specification (i.e., latency, TPU) is significantly various [5] and to train a global model without sharing local data. Federated learning (FL) is one of the most popular paradigms of collaborative machine learning [45; 35; 15; 34; 25; 46; 39; 1]. In general, to train the central server (e.g., service manager) in the FL framework, each client (e.g., mobile devices or whole organization) updates its local model via their private data by itself; all local updates are aggregated to the global model; after which the procedure is repeated until convergence. Most notably, federated averaging (FedAvg) [45] uses averaging as its aggregation method over the local learned models on clients. Such FL framework ensures us to occlude many of the systematic privacy leakages [57].

Recent FL works have been evolving into designing new objective functions for the aggregation of each model [1; 25; 34; 60; 13; 71; 31], using auxiliary data in the center server [39; 73], encoding the weight for an efficient communication stage [63; 23; 65], or recruiting helpful clients for more accurate global model [35; 8; 48]. On the other side, there has been tremendous recent interest in deploying the FL algorithms for real-world applications such as mobile devices and the Internet of

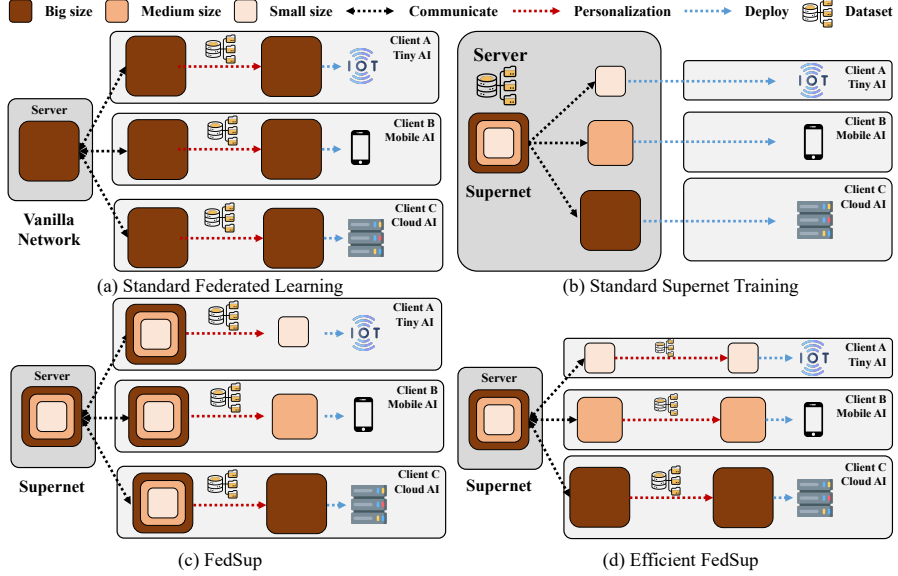


Figure 1: Overview of (a) standard FL framework, (b) supernet training in a standard datacenter optimization (i.e., centralized settings), (c) our proposed federation of supernet training framework (FedSup), and (d) efficient FedSup algorithm (E-FedSup).

Things (IoT) [48; 9; 18; 23]. However, less has been tackled on the issue of delivering compact models specialized for the edge device having different hardware platforms and efficiency constraints (Figure 1 (a)). It is known that the inference time of a neural network varies greatly depending on the specification of devices [70]. It would become a significant bottleneck at every aggregation round in FL’s synchronous training if a same-size model is distributed to clients without considering local resources [33].

Neural architecture search (NAS) studies have also suffered from such model heterogeneity issues in deploying resource-adaptive models to clients, but have resolved this challenge by training a single set of shared weight from one-shot models [5; 69; 59] (Figure 1 (b)). However, it has been under-explored under data-heterogeneity scenarios that can provoke the training instability. Recently, some works have studied the model heterogeneity in FL by sampling/generating a sub-network [47; 9; 53] or using a pruned model from a global model [18; 43]. Such methods have limitations on model scaling (e.g., depth (#layers), width (#channels), kernel size), training stability, and personalization of each clients.

This paper presents a novel framework to consider both scenarios, namely *Federation of Supernet Training* (FedSup) which encompasses the training of sub-models nested in a supernet under system heterogeneity. Using the weight-sharing in supernet training, FedSup forwards a supernet to each local client and ensembles the training of sub-models sampled from itself at each client (Figure 1 (c)). Referred to Diao et al. [9], we manifest a *Efficient FedSup* (E-FedSup) broadcasting a sub-model to local in lieu of a full supernet (Figure 1 (d)). For the evaluation of both methods, we focus on improving the global accuracy (of the server; universality) and the personalized accuracies (of on-device fine-tuned models; personalization). Our key contributions are summarized as follows:

- We propose a novel framework that obtains a large number of sub-networks at once, tackling the processing capabilities of local clients. We further develop an efficient version that broadcasts sub-models for local training - and thus diminishing the network bandwidth of clients (communication costs) and the local training overhead (local computational costs).
- Extending previous methods, we analyze the global accuracy and a personalized accuracy of each client in a situation where multiple dimensions (depth, width, kernel size) are dynamic. In addition, we show the superiority of our methods through accuracy vs. FLOPs Pareto.
- Our proposed solutions address various heterogeneous settings on several FL benchmark dataset, including medical dataset. We thoroughly study and revisit conventional training techniques of stand-alone networks for plugging into our framework.
- Our results demonstrate that both **FedSup** and **E-FedSup** bring more enhanced representations than those of other static training approaches, and thus improve both the global model’s accuracy and the personalized accuracy of each client.

Organization. The remainder of this paper is organized as follows. In Section 2, we discuss the recent literature on model-heterogeneity in FL and supernet training in NAS. In Section 3, we address our motivation for collaborating the federated learning with supernet training and provide our main methods, the Federation of Supernet Training (FedSup) and efficient FedSup (E-FedSup). In Section 4, we exhibit the experimental results. Finally, Section 5 concludes the paper.

2 Related Work

Designing specialized DNNs for every scenario is labor-intensive and computationally prohibitive with human-based methods or sample-based NAS [40]. Such methods require repeating the network design process and replacing the network design process from scratch in each case, and therefore their total cost increases linearly as the number of deployment scenarios increases. Furthermore, in the presence of a federated environment, such design cost is also significantly affected by the number of participating clients and the amount of each local data, even considering the network bandwidth of clients. To mitigate such issues, some works attempt to examine the single-shot model under data heterogeneity. We do not consider the works that assumed the availability of proxy data in the server [39; 73].

Dynamic Neural Network. Compared to static neural networks, dynamic neural networks can adapt their structures or parameters to the input during inference considering the quality-cost trade-off [16]. To adaptively allocate computations on demand at inference, some works selectively activate model components (e.g., layers [21], channels [38; 51]); a controller or gating modules are learned to dynamically choose which layers of a deep network [64; 41; 62]; Kuen et al. [30] introduce stochastic downsampling points to adaptively reduce the size of the feature map. By extending the capabilities of already-developed human-designed neural networks like the MobileNet series [19; 52], Slimmable nets [70; 68] train a model to support multiple width multipliers (for instance, 4 different global width multipliers).

Supernet. Supernet, a category of dynamic neural networks, assembles all candidate architectures into a weight-sharing network where each architecture corresponds to one sub-network. It is an emerging research topic in deep learning, specifically neural architecture search. It dramatically reduces the huge cost of searching, training, or fine-tuning each architecture individually whose child models can be directly deployed. Despite its strength, supernet training is highly challenging [70; 68]. For the stability of training optimization, it requires many training techniques such as (1) inplace knowledge distillation [68] leveraging the soft prediction of the largest sub-network for the supervision of other sub-networks, (2) modified batch normalization to synchronize the batch statistics of all child models [70; 68], (3) sampling strategy of child models from the supernet [5; 59], and (4) modified loss/gradient function [69; 58].

Benefits of Supernet. Many applications present the use cases of supernet for real-world scenarios. One of the most notable advantages is that they are able to allocate the user-customized network in consideration of their capabilities on edge devices (e.g., smartphones, the internet of things) [6]. Next, the supernet seemingly produces better representation power than the static version of the network [66; 5]. In addition, supernet alleviates the issue of excessive energy consumption and CO₂ emission caused by designing specialized DNNs for every scenario [54; 5]. Lastly, supernet has superior transferability across different datasets [74] and tasks [50; 14]. All these advantages seem like a double line that will work well in a federated environment, to our best knowledge, but there are few studies applied in FL yet. Recently, Diao et al. [9] show the possibility of coordinatively training local models by using a weight-sharing concept while it limits the degree of flexibility (e.g., only width multiplier can adapt), analysis of model behavior, the examination for a collection of training refinements, and the investigation towards personalization.

Model Heterogeneity in FL. Model heterogeneity in FL, the problem of training heterogeneous local models with varying computation complexities, has remained largely under-explored in comparison with statistical data heterogeneity. Recently, a few works have been proposed in the following direction: generating a set of sub-models through a hypernetwork that outputs parameters for other neural networks [53], using a pruned model from a global model [3; 18; 43], and distilling the knowledge from local to global by using either extra proxy datasets or generator [39; 2]. However, pruning approaches are not really cost-effective in terms of inference time, and distillation-based methodologies require additional training overhead. Using a hypernetwork [53] or sampling a sub-model from the global model [9] may avoid such issues, but the sub-model scale is limited to only a single direction such as width or kernel size. Furthermore, such optimization is simple so that

the accuracy gap among sub-models should be bridged through some advanced training techniques. Newly, Mushtaq et al. [47] apply continuous differentiable relaxation and gradient descent, but it is significantly sensitive to hyperparameter choices.

Personalized FL. Machine learning-based personalization has emerged for keeping privacy and fairness as well as recognizing the local particular character. Personalized federated learning has been proposed as one of them to learn personalized local models. To improve the performance, the methods for the personalized FL models have been evolving in such directions [56; 44; 49]: user clustering, designing new loss functions, meta-learning, and model interpolation. With meta-features from all clients, each local client is clustered by measuring the data distribution and sharing separate models for each cluster without inter-cluster federation [4; 44]. Adding a regularizer to the loss function can be a recommended scheme to prevent local models from overfitting their own local data [56; 32]. Bi-level optimization between clients and servers can be interpreted as *meta-learning* (i.e., Model-Agnostic Meta-Learning (MAML)). This approach aims to obtain a well-initialized shared global model that facilitates personalized generalization with a few fine-tuning [24; 49]. Lastly, decoupling the base and personalized layers in a network is used; both types of layers are trained by clients in addition to the server’s base layers to create a model that is unique to each user [49; 7]. On the other hand, few studies have been on personalized FL performance under the client system heterogeneity, which denotes the clients with different computational capabilities.

3 Method

3.1 Problem Settings: Federated Learning

The main goal of FL [45] is to solve the following optimization problem having distributed collection of heterogeneous data:

$$\min_{\mathbf{w}} f(\mathbf{w}) \triangleq \min_{\mathbf{w}} \sum_{k \in S} p_k F_k(\mathbf{w}) \quad (1)$$

where S is the set of total clients, p_k is the weight of client k , such as $p_k \geq 0$, and $\sum_k p_k = 1$. The local objective of client k is to minimize $F_k(\mathbf{w}) = \mathbb{E}_{\mathbf{x}_k \sim \mathcal{D}_k} [\ell_k(\mathbf{x}_k, \mathbf{y}_k; \mathbf{w})]$ parameterized by \mathbf{w} on the local data $(\mathbf{x}_k, \mathbf{y}_k)$ from local data distribution \mathcal{D}_k . FedAvg [45], the canonical algorithm for FL, involves *local update*, which learns a local model \mathbf{w}_k^t (Eq. 2) with learning rate η and synchronizing \mathbf{w}_k^t with \mathbf{w}^t every E steps,

$$\mathbf{w}_k^t \triangleq \begin{cases} \mathbf{w}_k^{t-1} - \eta \nabla F_k(\mathbf{w}_k^{t-1}) & \text{if } t \bmod E \neq 0 \\ \mathbf{w}^t & \text{if } t \bmod E = 0 \end{cases} \quad (2)$$

and *global aggregation*, which learns the global model \mathbf{w}^t (Eq. 3) by averaging all \mathbf{w}_k^t with regard to the client $k \in S^t$ uniformly sampled at random where p_k is used as $\frac{|\mathcal{D}_k|}{|\mathcal{D}|}$.

$$\mathbf{w}^t = \sum_{k \in S^t} p_k \mathbf{w}_k^t \quad (3)$$

3.2 Motivation for Weight Sharing in Client System Heterogeneity

Weight-sharing NAS is an effective technique for assembling all the architectures as its sub-networks and jointly trains the supernet [5; 69; 59; 58]. With the access permission to local data from the center server, it can be used for tackling the client system heterogeneity, the diversity in the processing capabilities and network bandwidth of clients, but not vice versa. Assuming the weights of the supernet as \mathbf{w} and the sub-models \mathbf{w}_{arch} , then the problem is generally formulated as follows:

$$\min_{\mathbf{w}} \sum_{\mathbf{w}_{arch} \subset \mathbf{w}} \mathbb{E}_{\mathbf{x} \sim \mathcal{D}} [\ell(\mathbf{x}, \mathbf{y}; \mathbf{w}_{arch})] \quad \text{where } \mathcal{D} = \bigcup_k \mathcal{D}_k \quad (4)$$

To preserve the data privacy, Eq. 4 can be reformulated with a simple double summation:

$$\begin{aligned} &= \min_{\mathbf{w}} \sum_{\mathbf{w}_{arch} \subset \mathbf{w}} \sum_k p_k \mathbb{E}_{\mathbf{x} \sim \mathcal{D}_k} [\ell_k(\mathbf{x}_k, \mathbf{y}_k; \mathbf{w}_{arch})] \\ &= \min_{\mathbf{w}} \sum_k p_k \sum_{\mathbf{w}_{arch} \subset \mathbf{w}} F_k(\mathbf{w}_{arch}) \end{aligned} \quad (5)$$

Algorithm 1: Generic Framework for FedSup

INPUT : Supernet w , the number of sampled child models M , weight update function UPDATE

- 1: Initialize SuperNet w_0
- 2: **for** $t \leftarrow 0, \dots, T - 1$ **do**
- 3: $S^t \leftarrow \text{SAMPLECLIENTS}$
- 4: **for** each client $k \in S^t$ in parallel **do**
- 5: $w_k^{t,0} \leftarrow w^t$ ▷ Broadcast a supernet w^t to client k
- 6: **for** $e \leftarrow 0, \dots, E - 1$ **do**
- 7: **for** $m = 1, \dots, M$ **do**
- 8: $w_{\text{arch}_{k,m}}^{t,e} \leftarrow \text{SAMPLEMODEL}(w_k^{t,e})$
- 9: $w_{\text{arch}_{k,m}}^{t,e+1} \leftarrow \text{OPTIMIZE}(w_{\text{arch}_{k,m}}^{t,e})$
- 10: **end for**
- 11: $w_k^{t,e+1} \leftarrow \text{UPDATE}(w_{\text{arch}_{k,1}}^{t,e+1}, \dots, w_{\text{arch}_{k,M}}^{t,e+1})$ ▷ Supernet optimization
- 12: **end for**
- 13: **end for**
- 14: $w^{t+1} \leftarrow \sum_{k \in S^t} p_k w_k^{t,E}$ ▷ Aggregation stage
- 14: **end for**

After exchanging the order of two summations, a new objective (Eq. 5) is obtained, termed as Federation of Supernet Training (FedSup) (Algorithm 1). Obviously, it is highly non-trivial due to the distinct learning dynamics of various child models under data heterogeneity; training strategies are mainly discussed in subsection 3.3.

Considerable efforts have been devoted to solving the efficiency problems of client system heterogeneity, which can be categorized into three dimensions as shown in Figure 2. We aim to design a robust framework to combine the federated averaging scheme with weight sharing on mobile-friendly architectures. We attempt to apply several training techniques to bridge the gap among three dimensions (Figure 2).

3.3 Training Strategies for FedSup

Architecture Space The details of our search space are presented by referring to the previous NAS and FL approaches [5; 69; 49]. Our network architecture consists of a stack with the MobileNet V1 blocks [19], and the detailed search space is summarized in Appendix. The arbitrary numbers of layers, channels, and kernel sizes can be sampled from our network. Following previous settings [70; 69], *lower-index layers* in each network stage are always kept. Both kernel size and channel numbers can be adjusted in a layer-wise manner.

Static Batch Normalizaiton. We follow the batch normalization settings used in the previous works [70; 9]. Specifically, because the running statistics of batch normalization layers can not be accumulated during training owing to the violence of data privacy as well as different model size [22], track running statistics are not tracked and simply normalized through the batch data. For the evaluation, BN statistics are updated as the local data is sequentially queried.

Inplace Distillation. During the FedSup training, a sub-model can be distilled with the soft labels predicted by the full model (biggest child), called *inplace distillation* [70]. Without any additional models, it can supervise a sub-model’s representation aligning into the same direction (i.e., *representation alignment*; a concept from Kim et al. [27]). The temperature hyperparameter and the balancing hyperparameter between distillation and target loss [17] are not used in our experiments.

M Sampled Child Models and Sandwich Rule. At every local training iteration, the gradients are aggregated from M sampled child models. If $M \geq 3$, the smallest child and the biggest child

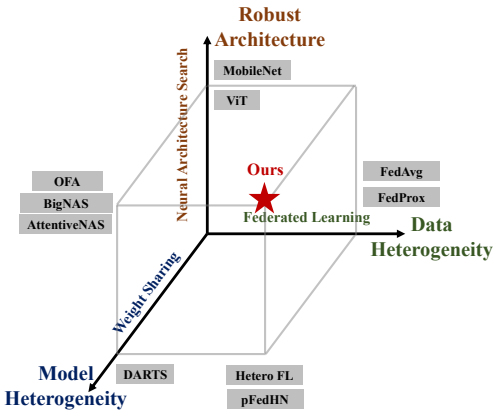


Figure 2: Illustration for the problem settings.

are included where the gradients are clipped (i.e., *sandwich rule* [70; 69]). Through these aggregated gradients, a supernet’s weight is updated where the “smallest” child denotes the model having the thinnest width, shallowest depth, and smallest kernel size under the pre-defined architecture space.

3.4 Efficient FedSup (E-FedSup)

If inplace distillation and sandwich rule are not applied during the local training, an alternative objective function can be used instead of Eq. 5:

$$\underbrace{\min_{\mathbf{w}} \sum_k p_k \sum_{\mathbf{w}_{arch} \subset \mathbf{w}} F_k(\mathbf{w}_{arch})}_{\text{FedSup}} \geq \underbrace{\min_{\mathbf{w}} \sum_k p_k F_k(\mathbf{w}_{arch_k})}_{\text{E-FedSup}} \quad \text{where } \mathbf{w}_{arch_k} \subset \mathbf{w} \quad (6)$$

In the broadcast stage, a sub-model is sent to each local client to achieve the efficiency on network bandwidth. A chief difference in the optimization is that FedSup samples a new sub-model every iteration, but E-FedSup trains a pre-fixed sub-model received during communication at local. E-FedSup saves communication cost by sending the child locally, and also curtails training overhead because it trains one model per iteration in lieu of several child models.

4 Experiment

4.1 Experimental Settings

Datasets We use three image classification benchmark datasets: CIFAR-10, CIFAR-100 [29], and pathMNIST for colon pathology classification, a collection of standardized biomedical images [67].

Heterogeneous Distribution of Client Data. We conduct two different kinds of heterogeneous data distribution settings referring to the literature [45; 49; 39]. Firstly, data is divided into the same-sized shards by considering its label distribution. Because there is no overlapping data between shards, the size of a shard is defined by $\frac{|D|}{N \times s}$, where $|D|$ is the data set size, N is the total number of clients, and s is the number of shards per user. In another way, we use the Dirichlet distribution to create disjoint non-i.i.d. (i.e., non-independent and identically distributed) client training data [72; 20; 39]. The amount of non-i.i.d.ness is determined by the value of β : $\beta = 100$ simulates identical local data distributions, and the lower the β , the more likely it is that the clients will only hold examples from one class (randomly chosen).

Training Details. To evaluate the personalized accuracy, each client has the same label distribution on local training and test data. Referred to Oh et al. [49], we control FL environments with following hyperparameters: client fraction ratio f , local epochs τ , shards per user s , and Dirichlet concentration parameter β . f is the number of participating clients out of the total number of clients in every round and a small f is natural in the FL settings because the total number of clients is numerous. We use the linear warmup learning rate scheduler until 20 rounds, and after warm-up, the learning rate is scheduled via cosine learning rate scheduler that is initialized with 0.1. Other settings not mentioned are followed by Oh et al. [49]. For the FedSup training, we use the number M of randomly sampled child model as equal to 3 and apply the inplace distillation. "Big (B)", "Medium (M)", "Small (S)" indicate the amount of FLOPS of sub-model sampled from the supernet located in the Pareto-frontier.

Evaluation. We evaluate the quality of both the global model and local models. For the evaluation of the global model, the whole test dataset is utilized for the global accuracy. For that of local models, we refer to as in Wang et. al. [61] and Oh et. al. [49]. Such personalization evaluation of each client is measured over two folds: (1) the transmitted global model is evaluated on each client having their own test dataset D_i^{ts} (referred to as the *initial accuracy*), (2) each local model is fine-tuned on its own training dataset D_i^{tr} with the fine-tuning epochs of τ_f ; such personalized model is then evaluated on its own test dataset of each client D_i^{ts} (referred to as the *personalized accuracy*). The values $(X_{\pm Y})$ in all tables indicate the mean \pm std of the accuracies across all clients, not across multiple seeds.

Table 1: Personalized accuracy on CIFAR-100 with 100 clients, $s = 50$, $f = 0.1$, and $m = 0.5$. A full supernet (Big) with dynamic width is utilized while the static version is applied on other algorithms.

Algorithm	Local-Only	FedAvg [45]	Ditto [32]	LG-FedAvg [36]	Per-FedAvg [12]	FedSup	E-FedSup
Personalized Acc.	27.98 ± 4.12	49.61 ± 5.10	44.10 ± 5.75	39.92 ± 5.02	44.21 ± 6.23	56.51 ± 5.15	55.75 ± 5.61

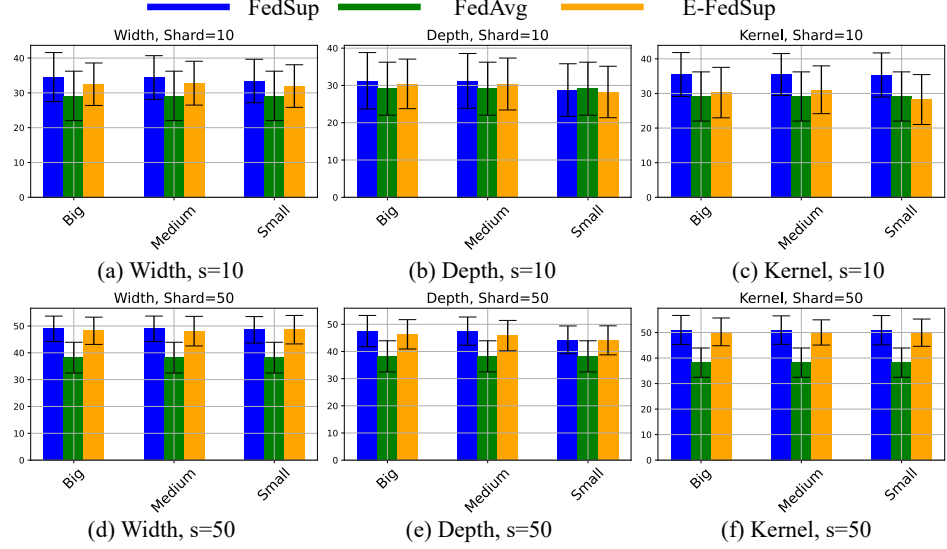


Figure 3: Global accuracies by changing the slimmability with network width, depth, and kernel size. Blue line indicates the FedSup training, the green line indicates the FedAvg [45] training and the orange line indicates the E-FedSup training. A static network (biggest child of supernet) is used for FedAvg while FedSup families are dynamic version (i.e., individually trained networks and slimmable networks have the same configurations (width, depth, and kernel size)).

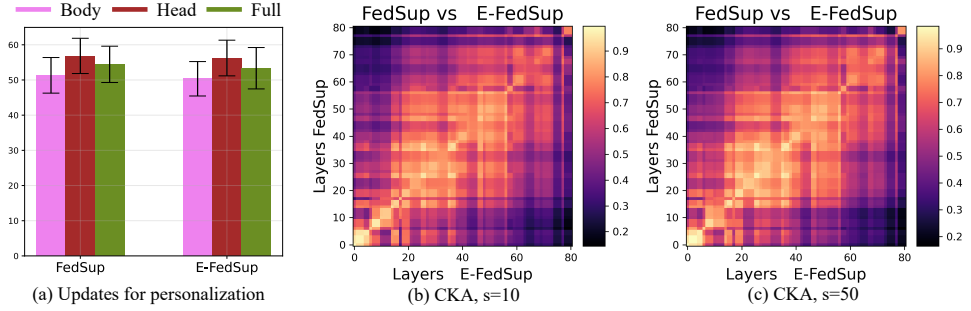


Figure 4: (a) Personalization accuracy of FedSup and E-FedSup on CIFAR-100 according to the fine-tuned part by referring to Oh et al. [49] (other parts are freezed); (b), (c): Centered Kernel Alignments (CKA) similarities of two different global models trained with FedSup and E-FedSup [28].

4.2 Evaluation on the Common Federated Learning Settings

Elastic Dimensions. We firstly take a closer look at applying the dynamic operations under federated settings towards three different dimensions: width, depth, and kernel size of convolutional operators. As Figure 3 shows, in most cases, FedSup and E-FedSup with any size of child networks outperforms the FedAvg using the static biggest network of supernet. Along any dimension, all child models are stably trained and produce more enhanced representations than those of static version models trained with FedAvg. The results of dynamic depth show little improvement in performance compared to those with dynamic width or kernel size, and in some cases its performance is lower than those of FedAvg, but it is marginal. This characteristic is desirable to extend the dimensions of model scale for the optimization.

Personalization. Referring to recent personalized FL experimental settings [49], we compare the performance according to the fine-tuned part (Figure 4 (a)). Child models are fine-tuned with five epochs based on the local training data. As mentioned in literature [49; 42], it is shown that updating only head has slightly better performance than the others including local-only training (Table 1). In the remaining paper, we thus update only the head for the personalization unless otherwise mentioned.

CKA Similarities [28]. We vividly compare how the representations of neural networks are changed through the FedSup and E-FedSup. To be specific, Centered Kernel Alignment (CKA) is leveraged to analyze the features learned by two architectures trained with FedSup and E-FedSup under different heterogeneous settings, given the same input testing samples (Figure 4 (b) and (c)).

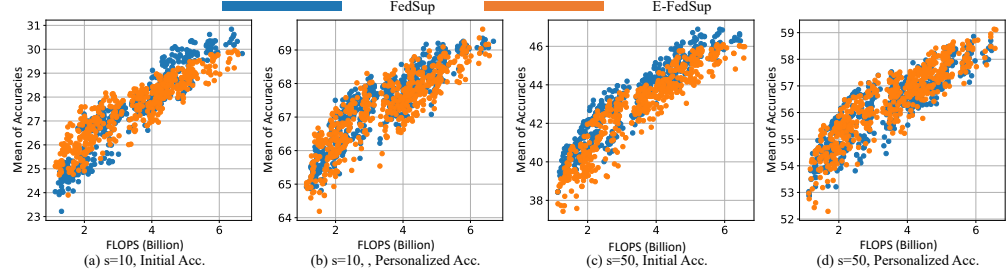


Figure 5: Attributes (e.g., initial acc., personalized acc., and FLOPS) of training process. Each dot represents a sub-model and 500 child models are sampled from the supernet.

Table 2: Initial and personalized accuracy on CIFAR100 under various FL settings with 100 clients. The initial and personalized accuracy indicate the evaluated performance without fine-tuning and after five fine-tuning epochs for each client, respectively.

FL Settings	s=50								s=10											
	f	τ	A	FedSup				E-FedSup				FedSup				E-FedSup				
				Initial	Personalized	Initial	Personalized	Initial	Personalized	Initial	Personalized	Initial	Personalized	Initial	Personalized	Initial	Personalized			
1.0	1	B	42.83 \pm 5.05	55.03 \pm 4.95	42.46 \pm 5.60	55.95 \pm 6.03	25.96 \pm 6.47	65.75 \pm 6.05	26.33 \pm 6.37	66.44 \pm 6.83	5	M	41.39 \pm 5.33	55.33 \pm 4.53	42.15 \pm 5.57	55.91 \pm 5.57	26.04 \pm 6.28	65.59 \pm 6.00	26.50 \pm 6.70	66.50 \pm 7.01
		M	39.19 \pm 4.77	53.17 \pm 4.77	39.78 \pm 5.29	54.35 \pm 5.88	25.06 \pm 5.94	64.81 \pm 6.12	25.20 \pm 6.00	64.53 \pm 6.52			40.33 \pm 5.02	52.78 \pm 5.66	40.22 \pm 5.28	53.24 \pm 5.42	25.01 \pm 5.11	66.49 \pm 6.36	26.41 \pm 5.97	66.30 \pm 6.34
		S	39.19 \pm 4.77	53.17 \pm 4.77	39.78 \pm 5.29	54.35 \pm 5.88	25.06 \pm 5.94	64.81 \pm 6.12	25.20 \pm 6.00	64.53 \pm 6.52			47.08 \pm 5.14	58.15 \pm 6.14	46.18 \pm 5.68	58.04 \pm 5.62	31.24 \pm 5.66	69.42 \pm 6.69	29.77 \pm 6.22	69.47 \pm 6.35
	0.1	B	38.94 \pm 5.30	53.55 \pm 4.81	39.37 \pm 5.40	54.88 \pm 4.79	22.43 \pm 5.11	65.12 \pm 5.95	22.42 \pm 5.32	64.75 \pm 6.38			38.09 \pm 5.40	53.31 \pm 5.26	39.33 \pm 5.10	54.81 \pm 5.22	22.40 \pm 5.23	64.95 \pm 6.21	22.23 \pm 5.66	64.73 \pm 6.55
		M	36.01 \pm 5.50	52.29 \pm 4.91	37.34 \pm 5.26	53.08 \pm 5.20	21.17 \pm 5.67	64.18 \pm 6.52	21.32 \pm 5.59	64.29 \pm 6.69			43.83 \pm 6.20	56.51 \pm 5.15	43.53 \pm 6.22	55.75 \pm 5.61	26.07 \pm 6.58	68.09 \pm 6.22	24.56 \pm 7.35	67.68 \pm 6.49
		S	37.94 \pm 5.15	52.15 \pm 5.28	37.19 \pm 5.10	52.33 \pm 5.38	20.27 \pm 6.98	64.41 \pm 6.30	20.28 \pm 6.71	64.35 \pm 5.99			42.21 \pm 5.78	55.42 \pm 5.35	42.24 \pm 5.72	55.38 \pm 5.51	24.81 \pm 6.99	67.93 \pm 6.32	24.76 \pm 7.23	67.87 \pm 6.50

Regardless of the degree of heterogeneity, CKA visualizations show that the representations of two neural networks trained with FedSup and E-FedSup seem similar during the propagation.

Compounding Dimensions. Table 2 describes the initial and personalized accuracies when combining the dimensions for architecture space. In most cases, FedSup has slightly less generalization error than E-FedSup in the global model (initial accuracy) while the personalized accuracy becomes almost similar when the five fine-tuning epochs are applied. Both FedSup and E-FedSup show a slight decrease in performance as a model size gets smaller.

Pareto Frontier. We compare the accuracy vs. FLOPS Pareto that finds the set of solutions where improving one objective will degrade another in the Multi-Objective Optimization [11]. Here, we randomly sample 500 sub-models from the supernet and estimate their initial and personalized accuracies. As Figure 5 shows, FedSup has better Pareto frontier than E-FedSup for the initial accuracy while Pareto frontiers for personalized accuracy are almost similar.

Inference Time. Figure 6 shows the results of the boxplot plotting sub-models’ inference time comparing with other model heterogeneity methods FjORD [18] and HeteroFL [9]. We demonstrate that FedSup spawns much more efficient models in terms of local inference time. Because FjORD and HeteroFL are either unstructured pruning or channel pruning-based methodologies, ours have lower processing time benefitted from dynamic depth. We measure the inference time on the NVIDIA 2080-Ti GPU.

4.2.1 Ablation Studies: Momentum and Label Smoothing

Momentum. Table 3 describes the initial and personalized accuracy according to the momentum. The momentum is not applied during the fine-tuning of personalization. In most cases, appropriate momentum improves the performance.

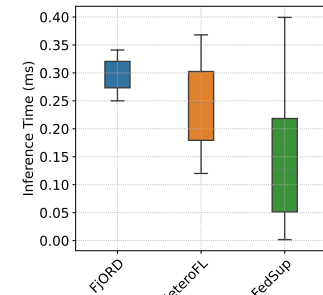


Figure 6: Comparison of other model heterogeneity methods about the inference time per image of each sub-model.

Table 3: Initial and personalized accuracy of FedSup and E-FedSup on CIFAR-100 according to the change of the momentum magnitude. The fine-tuning epochs is 5, f is 0.1, N is 100, and s is 10.

Settings		B		M		S	
Alg.	m	Initial	Personalized	Initial	Personalized	Initial	Personalized
FedSup	0.0	31.76 \pm 7.07	68.92 \pm 6.18	31.73 \pm 7.54	68.43 \pm 6.26	31.24 \pm 7.47	67.39 \pm 7.28
	0.1	32.52 \pm 6.45	68.03 \pm 5.95	32.09 \pm 6.94	68.51 \pm 5.96	31.41 \pm 6.62	66.92 \pm 5.91
	0.5	34.54 \pm 7.04	69.98 \pm 6.89	34.40 \pm 6.29	70.83 \pm 6.11	33.40 \pm 6.25	68.34 \pm 6.89
E-FedSup	0.0	32.67 \pm 6.80	67.61 \pm 6.81	32.69 \pm 6.80	67.74 \pm 7.05	32.19 \pm 6.62	66.30 \pm 7.22
	0.1	32.78 \pm 6.88	67.69 \pm 6.19	32.93 \pm 7.05	67.33 \pm 6.28	32.23 \pm 6.64	66.02 \pm 6.65
	0.5	32.49 \pm 6.10	68.50 \pm 7.38	32.79 \pm 6.30	68.77 \pm 6.83	31.96 \pm 6.12	66.81 \pm 6.88

Table 4: Initial and personalized accuracy of FedSup and E-FedSup on CIFAR-100 with and without label smoothing. The fine-tuning epochs is 5, f is 0.1, N is 100, and s is 10.

Architecture Size		B		M		S	
Architecture	LS	Initial	Personalized	Initial	Personalized	Initial	Personalized
FedSup	0.0	34.54 \pm 7.04	69.98 \pm 6.89	34.40 \pm 6.29	70.83 \pm 6.11	33.40 \pm 6.25	68.34 \pm 6.89
	0.1	31.44 \pm 6.89	68.92 \pm 7.48	31.34 \pm 7.03	68.56 \pm 7.25	30.81 \pm 7.28	66.90 \pm 7.60
E-FedSup	0.0	32.49 \pm 6.10	68.50 \pm 7.38	32.79 \pm 6.30	68.77 \pm 6.83	31.96 \pm 6.12	66.81 \pm 6.88
	0.1	31.89 \pm 6.98	68.71 \pm 6.45	31.70 \pm 6.48	68.35 \pm 6.88	30.64 \pm 6.91	65.77 \pm 6.71

Label Smoothing (LS) [55]. Table 4 describes the initial and personalized accuracy according to the LS. LS is popularly used in the existing weight-sharing methods [5; 69; 59], but in our environment, it rather degrades both initial and personalized performance.

4.2.2 Experiments on Medical Dataset

As Table 5 shows, FedSup and E-FedSup work fairly well on the PathMNIST dataset and have the similar tendency presented in Table 2.

Table 5: Initial and personalized accuracy on PathMNIST [67] under various FL settings with 100 clients. We implement data heterogeneity through Dirichlet distribution (β) [72; 20; 39]. FedAvg algorithm has 2-3% lower initial and personalized acc. on average than E-FedSup (Appendix).

FL Settings		$\beta = 100.0$				$\beta = 1.0$			
f	A	FedSup		E-FedSup		FedSup		E-FedSup	
		Initial	Personalized	Initial	Personalized	Initial	Personalized	Initial	Personalized
1.0	B	75.02 \pm 4.95	74.67 \pm 4.56	73.04 \pm 4.39	73.56 \pm 4.74	71.70 \pm 8.01	79.67 \pm 6.34	70.33 \pm 8.10	79.17 \pm 6.62
	M	74.33 \pm 4.45	74.33 \pm 4.40	74.30 \pm 4.47	73.69 \pm 4.66	70.19 \pm 7.91	78.63 \pm 6.84	69.40 \pm 8.43	78.48 \pm 7.33
	S	74.03 \pm 4.41	73.12 \pm 4.54	70.66 \pm 5.50	70.00 \pm 5.60	68.59 \pm 8.17	77.60 \pm 7.17	66.95 \pm 8.14	76.38 \pm 7.65
0.1	B	74.76 \pm 4.23	74.38 \pm 4.20	73.91 \pm 4.87	73.22 \pm 4.95	70.07 \pm 8.65	79.30 \pm 7.29	69.40 \pm 8.05	79.08 \pm 6.74
	M	73.97 \pm 4.90	73.48 \pm 4.54	74.08 \pm 4.91	73.26 \pm 4.54	69.46 \pm 9.23	78.80 \pm 6.33	69.13 \pm 9.07	78.76 \pm 6.24
	S	73.23 \pm 4.84	71.79 \pm 4.63	73.88 \pm 4.44	72.97 \pm 4.94	68.05 \pm 8.77	77.37 \pm 7.63	67.27 \pm 8.97	76.99 \pm 7.58

5 Conclusion

In this paper, motivated by the weigh-sharing utilized for the training of a supernet whereby it contains all possible architectures sampled from itself, we proposed a novel branch of approaches, termed FedSup (Federation of Supernet Training) under system heterogeneity. Our work engages in the solutions of federated learning for both data-heterogeneity and model-heterogeneity. Specifically, FedSup aggregates a large number of sub-networks with different capabilities into one global model at once. In addition, we further develop an efficient version of FedSup (E-FedSup) which reduces the model size transferred per round as well as local training overhead. We show that FedSup and E-FedSup have an excellent ability to generalize the personal data as well as the global data. Our methods yield strong results on standard benchmarks and a medical dataset for federated scenarios. Our methods can be applied to distributed learning to reduce network bandwidth as well as computation time on inference. Despite the promise of FL, it has been limited owing to the large bandwidth requirement and computational capabilities of each local device. We believe that our work opens the door to deploying resource-adaptive service access to real-world applications where the capabilities of systems are diverse. Also, the energy consumption from training costs is dramatically reduced. We believe that our contribution will lower the barriers to entry for developing dynamic FL models for DL practitioners and greatly impact the IoT industry.

References

- [1] Durmus Alp Emre Acar, Yue Zhao, Ramon Matas Navarro, Matthew Mattina, Paul N Whatmough, and Venkatesh Saligrama. Federated learning based on dynamic regularization. In *International Conference on Learning Representations*, 2021.
- [2] Andrei Afonin and Sai Praneeth Karimireddy. Towards model agnostic federated learning using knowledge distillation. In *International Conference on Learning Representations*, 2022.
- [3] Nader Bouacida, Jiahui Hou, Hui Zang, and Xin Liu. Adaptive federated dropout: Improving communication efficiency and generalization for federated learning. *CoRR*, abs/2011.04050, 2020.
- [4] Christopher Briggs, Zhong Fan, and Peter Andras. Federated learning with hierarchical clustering of local updates to improve training on non-iid data. In *2020 International Joint Conference on Neural Networks (IJCNN)*, pages 1–9. IEEE, 2020.
- [5] Han Cai, Chuang Gan, and Song Han. Once for all: Train one network and specialize it for efficient deployment. *CoRR*, abs/1908.09791, 2019.
- [6] Han Cai, Ligeng Zhu, and Song Han. Proxylessnas: Direct neural architecture search on target task and hardware. *arXiv preprint arXiv:1812.00332*, 2018.
- [7] Hong-You Chen and Wei-Lun Chao. On bridging generic and personalized federated learning for image classification. In *International Conference on Learning Representations*, 2021.
- [8] Yae Jee Cho, Jianyu Wang, and Gauri Joshi. Client selection in federated learning: Convergence analysis and power-of-choice selection strategies. *arXiv preprint arXiv:2010.01243*, 2020.
- [9] Enmao Diao, Jie Ding, and Vahid Tarokh. Hetero{fl}: Computation and communication efficient federated learning for heterogeneous clients. In *International Conference on Learning Representations*, 2021.
- [10] Hesham El-Sayed, Sharmi Sankar, Mukesh Prasad, Deepak Puthal, Akshansh Gupta, Manoranjan Mohanty, and Chin-Teng Lin. Edge of things: The big picture on the integration of edge, iot and the cloud in a distributed computing environment. *IEEE Access*, 6:1706–1717, 2018.
- [11] David Eriksson, Pierce I-Jen Chuang, Sam Daulton, Ahmed Aly, Arun Babu, Akshat Shrivastava, Peng Xia, Shicong Zhao, Ganesh Venkatesh, and Maximilian Balandat. Latency-aware neural architecture search with multi-objective bayesian optimization. *arXiv preprint arXiv:2106.11890*, 2021.
- [12] Alireza Fallah, Aryan Mokhtari, and Asuman Ozdaglar. Personalized federated learning with theoretical guarantees: A model-agnostic meta-learning approach. *Advances in Neural Information Processing Systems*, 33, 2020.
- [13] X Yu Felix, Ankit Singh Rawat, Aditya Krishna Menon, and Sanjiv Kumar. Federated learning with only positive labels. *arXiv preprint arXiv:2004.10342*, 2020.
- [14] Yuan Gao, Haoping Bai, Zequn Jie, Jiayi Ma, Kui Jia, and Wei Liu. Mtl-nas: Task-agnostic neural architecture search towards general-purpose multi-task learning. In *Proceedings of the IEEE/CVF Conference on Computer Vision and Pattern Recognition*, pages 11543–11552, 2020.
- [15] Pengchao Han, Shiqiang Wang, and Kin K Leung. Adaptive gradient sparsification for efficient federated learning: An online learning approach. *arXiv preprint arXiv:2001.04756*, 2020.
- [16] Yizeng Han, Gao Huang, Shiji Song, Le Yang, Honghui Wang, and Yulin Wang. Dynamic neural networks: A survey. *IEEE Transactions on Pattern Analysis and Machine Intelligence*, 2021.
- [17] Geoffrey Hinton, Oriol Vinyals, Jeff Dean, et al. Distilling the knowledge in a neural network. *arXiv preprint arXiv:1503.02531*, 2(7), 2015.

[18] Samuel Horvath, Stefanos Laskaridis, Mario Almeida, Ilias Leontiadis, Stylianos Venieris, and Nicholas Lane. Fjord: Fair and accurate federated learning under heterogeneous targets with ordered dropout. *Advances in Neural Information Processing Systems*, 34, 2021.

[19] Andrew G Howard, Menglong Zhu, Bo Chen, Dmitry Kalenichenko, Weijun Wang, Tobias Weyand, Marco Andreetto, and Hartwig Adam. Mobilenets: Efficient convolutional neural networks for mobile vision applications. *arXiv preprint arXiv:1704.04861*, 2017.

[20] Tzu-Ming Harry Hsu, Hang Qi, and Matthew Brown. Measuring the effects of non-identical data distribution for federated visual classification. *arXiv preprint arXiv:1909.06335*, 2019.

[21] Gao Huang, Danlu Chen, Tianhong Li, Felix Wu, Laurens Van Der Maaten, and Kilian Q Weinberger. Multi-scale dense networks for resource efficient image classification. *arXiv preprint arXiv:1703.09844*, 2017.

[22] Yangsibo Huang, Samyak Gupta, Zhao Song, Kai Li, and Sanjeev Arora. Evaluating gradient inversion attacks and defenses in federated learning. In A. Beygelzimer, Y. Dauphin, P. Liang, and J. Wortman Vaughan, editors, *Advances in Neural Information Processing Systems*, 2021.

[23] Nam Hyeon-Woo, Moon Ye-Bin, and Tae-Hyun Oh. Fedpara: Low-rank hadamard product for communication-efficient federated learning. In *International Conference on Learning Representations*, 2022.

[24] Yihan Jiang, Jakub Konečný, Keith Rush, and Sreeram Kannan. Improving federated learning personalization via model agnostic meta learning. *arXiv preprint arXiv:1909.12488*, 2019.

[25] Sai Praneeth Karimireddy, Satyen Kale, Mehryar Mohri, Sashank J Reddi, Sebastian U Stich, and Ananda Theertha Suresh. Scaffold: Stochastic controlled averaging for on-device federated learning. *arXiv preprint arXiv:1910.06378*, 2019.

[26] Jakob Nikolas Kather, Johannes Krisam, Pornpimol Charoentong, Tom Luedde, Esther Herpel, Cleo-Aron Weis, Timo Gaiser, Alexander Marx, Nektarios A Valous, Dyke Ferber, et al. Predicting survival from colorectal cancer histology slides using deep learning: A retrospective multicenter study. *PLoS medicine*, 16(1):e1002730, 2019.

[27] Taehyeon Kim, Jongwoo Ko, Sangwook Cho, JinHwan Choi, and Se-Young Yun. FINE samples for learning with noisy labels. In A. Beygelzimer, Y. Dauphin, P. Liang, and J. Wortman Vaughan, editors, *Advances in Neural Information Processing Systems*, 2021.

[28] Simon Kornblith, Mohammad Norouzi, Honglak Lee, and Geoffrey Hinton. Similarity of neural network representations revisited. In *International Conference on Machine Learning*, pages 3519–3529. PMLR, 2019.

[29] Alex Krizhevsky, Geoffrey Hinton, et al. Learning multiple layers of features from tiny images. 2009.

[30] Jason Kuen, Xiangfei Kong, Zhe Lin, Gang Wang, Jianxiong Yin, Simon See, and Yap-Peng Tan. Stochastic downsampling for cost-adjustable inference and improved regularization in convolutional networks. In *Proceedings of the IEEE Conference on Computer Vision and Pattern Recognition*, pages 7929–7938, 2018.

[31] Qinbin Li, Bingsheng He, and Dawn Song. Model-contrastive federated learning. In *Proceedings of the IEEE/CVF Conference on Computer Vision and Pattern Recognition*, pages 10713–10722, 2021.

[32] Tian Li, Shengyuan Hu, Ahmad Beirami, and Virginia Smith. Ditto: Fair and robust federated learning through personalization. In *International Conference on Machine Learning*, pages 6357–6368. PMLR, 2021.

[33] Tian Li, Anit Kumar Sahu, Ameet Talwalkar, and Virginia Smith. Federated learning: Challenges, methods, and future directions. *IEEE Signal Processing Magazine*, 37(3):50–60, 2020.

[34] Tian Li, Anit Kumar Sahu, Manzil Zaheer, Maziar Sanjabi, Ameet Talwalkar, and Virginia Smith. Federated optimization in heterogeneous networks. *arXiv preprint arXiv:1812.06127*, 2018.

[35] Xiang Li, Kaixuan Huang, Wenhao Yang, Shusen Wang, and Zhihua Zhang. On the convergence of fedavg on non-iid data. *arXiv preprint arXiv:1907.02189*, 2019.

[36] Paul Pu Liang, Terrance Liu, Liu Ziyin, Nicholas B Allen, Randy P Auerbach, David Brent, Ruslan Salakhutdinov, and Louis-Philippe Morency. Think locally, act globally: Federated learning with local and global representations. *arXiv preprint arXiv:2001.01523*, 2020.

[37] Wei Yang Bryan Lim, Nguyen Cong Luong, Dinh Thai Hoang, Yutao Jiao, Ying-Chang Liang, Qiang Yang, Dusit Niyato, and Chunyan Miao. Federated learning in mobile edge networks: A comprehensive survey. *IEEE Communications Surveys Tutorials*, 22(3):2031–2063, 2020.

[38] Ji Lin, Yongming Rao, Jiwen Lu, and Jie Zhou. Runtime neural pruning. *Advances in neural information processing systems*, 30, 2017.

[39] Tao Lin, Lingjing Kong, Sebastian U Stich, and Martin Jaggi. Ensemble distillation for robust model fusion in federated learning. *arXiv preprint arXiv:2006.07242*, 2020.

[40] Hanxiao Liu, Karen Simonyan, and Yiming Yang. Darts: Differentiable architecture search. *arXiv preprint arXiv:1806.09055*, 2018.

[41] Lanlan Liu and Jia Deng. Dynamic deep neural networks: Optimizing accuracy-efficiency trade-offs by selective execution. In *Proceedings of the AAAI Conference on Artificial Intelligence*, volume 32, 2018.

[42] Mi Luo, Fei Chen, Dapeng Hu, Yifan Zhang, Jian Liang, and Jiashi Feng. No fear of heterogeneity: Classifier calibration for federated learning with non-iid data. *Advances in Neural Information Processing Systems*, 34, 2021.

[43] Mi Luo, Fei Chen, Zhenguo Li, and Jiashi Feng. Architecture personalization in resource-constrained federated learning. 2021.

[44] Yishay Mansour, Mehryar Mohri, Jae Ro, and Ananda Theertha Suresh. Three approaches for personalization with applications to federated learning. *arXiv preprint arXiv:2002.10619*, 2020.

[45] Brendan McMahan, Eider Moore, Daniel Ramage, Seth Hampson, and Blaise Aguera y Arcas. Communication-efficient learning of deep networks from decentralized data. In *Artificial Intelligence and Statistics*, pages 1273–1282, 2017.

[46] Mehryar Mohri, Gary Sivek, and Ananda Theertha Suresh. Agnostic federated learning. *arXiv preprint arXiv:1902.00146*, 2019.

[47] Erum Mushtaq, Chaoyang He, Jie Ding, and Salman Avestimehr. Spider: Searching personalized neural architecture for federated learning. *arXiv preprint arXiv:2112.13939*, 2021.

[48] Takayuki Nishio and Ryo Yonetani. Client selection for federated learning with heterogeneous resources in mobile edge. In *ICC 2019-2019 IEEE International Conference on Communications (ICC)*, pages 1–7. IEEE, 2019.

[49] Jaehoon Oh, Sangmook Kim, and Se-Young Yun. Fedbabu: Towards enhanced representation for federated image classification. *arXiv preprint arXiv:2106.06042*, 2021.

[50] Ramakanth Pasunuru and Mohit Bansal. Continual and multi-task architecture search. *arXiv preprint arXiv:1906.05226*, 2019.

[51] Sara Sabour, Nicholas Frosst, and Geoffrey E Hinton. Dynamic routing between capsules. *Advances in neural information processing systems*, 30, 2017.

[52] Mark Sandler, Andrew Howard, Menglong Zhu, Andrey Zhmoginov, and Liang-Chieh Chen. Mobilenetv2: Inverted residuals and linear bottlenecks. In *Proceedings of the IEEE conference on computer vision and pattern recognition*, pages 4510–4520, 2018.

[53] Aviv Shamsian, Aviv Navon, Ethan Fetaya, and Gal Chechik. Personalized federated learning using hypernetworks. In *International Conference on Machine Learning*, pages 9489–9502. PMLR, 2021.

[54] Emma Strubell, Ananya Ganesh, and Andrew McCallum. Energy and policy considerations for deep learning in nlp. *arXiv preprint arXiv:1906.02243*, 2019.

[55] Christian Szegedy, Vincent Vanhoucke, Sergey Ioffe, Jon Shlens, and Zbigniew Wojna. Rethinking the inception architecture for computer vision. In *Proceedings of the IEEE conference on computer vision and pattern recognition*, pages 2818–2826, 2016.

[56] Canh T Dinh, Nguyen Tran, and Josh Nguyen. Personalized federated learning with moreau envelopes. *Advances in Neural Information Processing Systems*, 33:21394–21405, 2020.

[57] Paul Voigt and Axel Von dem Bussche. The eu general data protection regulation (gdpr). *A Practical Guide, 1st Ed., Cham: Springer International Publishing*, 10(3152676):10–5555, 2017.

[58] Dilin Wang, Chengyue Gong, Meng Li, Qiang Liu, and Vikas Chandra. Alphanet: Improved training of supernets with alpha-divergence. In *International Conference on Machine Learning*, pages 10760–10771. PMLR, 2021.

[59] Dilin Wang, Meng Li, Chengyue Gong, and Vikas Chandra. Attentivenas: Improving neural architecture search via attentive sampling. In *Proceedings of the IEEE/CVF Conference on Computer Vision and Pattern Recognition*, pages 6418–6427, 2021.

[60] Jianyu Wang, Qinghua Liu, Hao Liang, Gauri Joshi, and H Vincent Poor. Tackling the objective inconsistency problem in heterogeneous federated optimization. *arXiv preprint arXiv:2007.07481*, 2020.

[61] Kangkang Wang, Rajiv Mathews, Chloé Kiddon, Hubert Eichner, Françoise Beaufays, and Daniel Ramage. Federated evaluation of on-device personalization. *arXiv preprint arXiv:1910.10252*, 2019.

[62] Xin Wang, Fisher Yu, Zi-Yi Dou, Trevor Darrell, and Joseph E Gonzalez. Skipnet: Learning dynamic routing in convolutional networks. In *Proceedings of the European Conference on Computer Vision (ECCV)*, pages 409–424, 2018.

[63] Chuhan Wu, Fangzhao Wu, Lingjuan Lyu, Yongfeng Huang, and Xing Xie. Communication-efficient federated learning via knowledge distillation. *Nature communications*, 13(1):1–8, 2022.

[64] Zuxuan Wu, Tushar Nagarajan, Abhishek Kumar, Steven Rennie, Larry S Davis, Kristen Grauman, and Rogerio Feris. Blockdrop: Dynamic inference paths in residual networks. In *Proceedings of the IEEE Conference on Computer Vision and Pattern Recognition*, pages 8817–8826, 2018.

[65] Hang Xu, Kelly Kostopoulou, Aritra Dutta, Xin Li, Alexandros Ntoulas, and Panos Kalnis. Deepreduce: A sparse-tensor communication framework for federated deep learning. *Advances in Neural Information Processing Systems*, 34:21150–21163, 2021.

[66] Brandon Yang, Gabriel Bender, Quoc V Le, and Jiquan Ngiam. Condconv: Conditionally parameterized convolutions for efficient inference. *Advances in Neural Information Processing Systems*, 32, 2019.

[67] Jiancheng Yang, Rui Shi, Donglai Wei, Zequan Liu, Lin Zhao, Bilian Ke, Hanspeter Pfister, and Bingbing Ni. Medmnist v2: A large-scale lightweight benchmark for 2d and 3d biomedical image classification. *arXiv preprint arXiv:2110.14795*, 2021.

[68] Jiahui Yu and Thomas S Huang. Universally slimmable networks and improved training techniques. In *Proceedings of the IEEE/CVF international conference on computer vision*, pages 1803–1811, 2019.

[69] Jiahui Yu, Pengchong Jin, Hanxiao Liu, Gabriel Bender, Pieter-Jan Kindermans, Mingxing Tan, Thomas Huang, Xiaodan Song, Ruoming Pang, and Quoc Le. Bignas: Scaling up neural architecture search with big single-stage models. In *European Conference on Computer Vision*, pages 702–717. Springer, 2020.

- [70] Jiahui Yu, Linjie Yang, Ning Xu, Jianchao Yang, and Thomas S. Huang. Slimmable neural networks. *CoRR*, abs/1812.08928, 2018.
- [71] Honglin Yuan and Tengyu Ma. Federated accelerated stochastic gradient descent. *arXiv preprint arXiv:2006.08950*, 2020.
- [72] Mikhail Yurochkin, Mayank Agarwal, Soumya Ghosh, Kristjan Greenewald, Trong Nghia Hoang, and Yasaman Khazaeni. Bayesian nonparametric federated learning of neural networks. *arXiv preprint arXiv:1905.12022*, 2019.
- [73] Lin Zhang, Li Shen, Liang Ding, Dacheng Tao, and Ling-Yu Duan. Fine-tuning global model via data-free knowledge distillation for non-iid federated learning. *arXiv preprint arXiv:2203.09249*, 2022.
- [74] Barret Zoph, Vijay Vasudevan, Jonathon Shlens, and Quoc V Le. Learning transferable architectures for scalable image recognition. In *Proceedings of the IEEE conference on computer vision and pattern recognition*, pages 8697–8710, 2018.

A Overview of Appendix

In this supplementary material, we present additional details, results, and experiments that are not included in the main paper due to the space limit.

B Ethics Statement

To address potential concerns, we describe the ethical aspect in respects to privacy, security, infrastructure level gap, and energy consumption.

Privacy and Security. Despite the promise of FL, owing to the presence of malicious users or the stragglers in the network, some workers may disturb the protocols and send arbitrary/adversarial messages that disturbs the generalization during FL. Recently, to tackle the system heterogeneity, some works allows the server to use proxy data or transmit encrypted data from local to server, but it may infringes on privacy. FedSup is also able to have such potential risks during communication. However, because FedSup can enable the training of models under heterogeneous system without using any proxy dataset, our methods could be used as a general solution to personalize the model, having less risks of privacy and security under system heterogeneity. Under adversarial attacks, it would be a nice direction to investigate the defense methods regarding the robustness against such adversarial risks.

Infrastructure Level Gap. In real-world applications, there is a bandwidth issues between clients and the server. More precisely, because of some limited-service access to areas where communication is rarely possible. Sending a model of the same size can greatly affect the synchronize training of FL with such infrastructure level gap. Because our work is efficient in terms of communication cost, we can deploy the model resource-adaptively. In addition, it is possible to use the model adaptively enough within the local according to the model resource and situation.

Energy Consumption. Our methods is more efficient than other methods in the respect of energy consumption: (1) communication efficiency and (2) design costs. Firstly, if E-FedSup is used, the sub-model is transferred to local as a substitute for the full supernet. Therefere, noticeable energy-saving effects can be obtained. On the other side, since our methods can design various architectures rather than specialized neural networks, our approach reduces the cost of specialized deep learning deployment from $O(N)$ to $O(1)$ [5]. Even, our methods has less generalization errors than other FedAvg-variant methods while total communication costs are the same, so further energy-savings can happen in the respect of convergence speed.

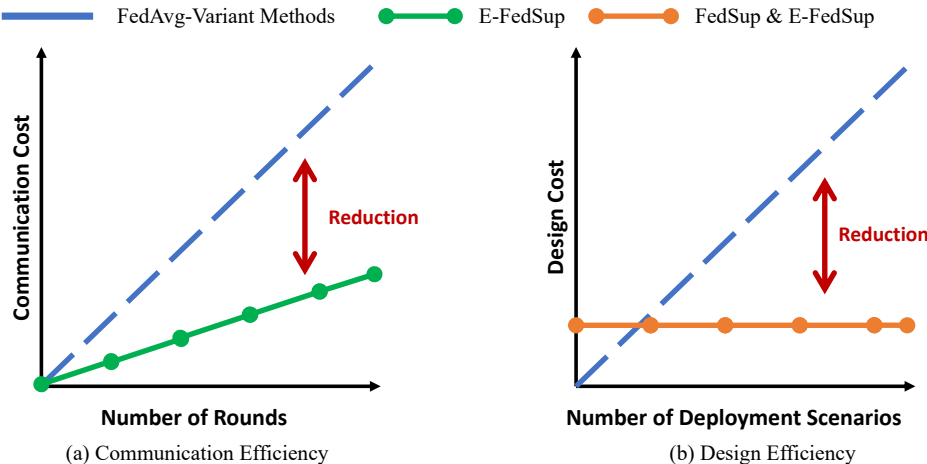


Figure 7: Savings of energy consumption in the respects to communication costs and design costs.

C Limitations and Future Directions

In this sections, we describe the limitations of our work and future directions for further development.

Limitations. Although illustrating the superiority of our proposed methods over state of the art, the bottleneck lies in the presence of arbitrary device unavailability or adversarial clients that disturbs the training. We only consider vision-centric classification tasks on smaller datasets (CIFAR-10, CIFAR-100, CINIC, PathMNIST). We do not investigate a large-scale datasets (namely ImageNet); FL framework gets computationally more prohibitive as the number of clients and local training iterations are increasing.

Future Directions. In future work, we aim to explore more efficient training strategies in the presence of stragglers and adversarial users. Furthermore, we improve the robustness of FedSup families in more resource-intensive settings. We intend to investigate our methods on other applications such as object-detection, semantic segmentation, and natural language processing models. Lastly, we plan to explore why FedSup and E-FedSup has similar personalization accuracies while the global accuracy has slight gap between FedSup and E-FedSup.

D Conceptual Comparison to Prior Works

Recently, numerous studies have been studied to address the problem of either data heterogeneity or model heterogeneity. As discussed in Section 2, literature can be categorized into several groups with FedSup and E-FedSup: data heterogeneity, model heterogeneity, and their hybrid. Table 6 systematically compares related methods in the respect to flexibility, data-privacy, efficiency on design, and efficiency on communication. More detailed explanations are described in Section 2. To the best of our knowledge, our methods are the first method to satisfy the two conflicting factors: *compounding model scales* (depth, width, kernel size) and *personalized models*, by taking advantage of both categories.

Table 6: Comparison with related training methods: each method is grouped into three categories. In the first row, "Flexibility": need not be tied with a specific architecture; "Data Privacy": keep the data privacy on each client; "Efficiency on Design": can design the architecture efficiently; "Efficiency on Communication": can reduce the communication cost between clients and the server.

Category	Data Heterogeneity			Model Heterogeneity		Hybrid
Method	FedAvg [45]	AFD [3]	FedDF [39]	OFA [5]	BigNAS [69]	Ours
Flexibility	X	X	O	O	O	O
Data-Privacy	O	O	O	X	X	O
Efficieny on Design	X	X	X	O	O	O
Efficiency on Communication	X	O	X	X	X	O

E Implementation Details for section 4

We build our methods and reproduce all experimental results referring to other official repositories^{1, 2, 3}.

E.1 Architectural Space

In this section, we present the details of our search space. Our network architectures consist of a stack with MobilenetV1 blocks (MBConv) [19]. The detailed search space is summarized in Table 7. For the depth dimension, our network has five stages (excluding the first convolutional layer (also called Stem)). Each stage has multiple choices of the number of layers, the number of channels and kernel size.

¹<https://github.com/facebookresearch/AttentiveNAS>

²<https://github.com/jhoon-oh/FedBABU>

³<https://github.com/pliang279/LG-FedAvg>

Table 7: MobileNetV1-based search space.

Stage	Operator	Resolution	#Channels	#Layers	Kernel Sizes
	Conv	32x32	32	1	3
1	MBCConv	16x16	32-64	1-1	3,5,7
2	MBCConv	16x16	64-128	1-2	3,5,7
3	MBCConv	8x8	128-256	1-2	3,5,7
4	MBCConv	4x4	256-512	3-6	3,5,7
5	MBCConv	2x2	512-1024	1-2	3,5,7

E.2 Experimental Settings

Data Preprocessing. We use the same settings in [49]. We apply normalization and simple data augmentation techniques (random crop and horizontal flip) on the training sets of all datasets. The size of the random crop is set to 32 for all datasets referred to previous works [49; 36; 45].

Dirichlet Distribution. To simulate a wide range of non-IIDness, we designed representative heterogeneity settings based on widely used techniques [72]. A dataset is partitioned by following $\mathbf{p}_c \sim Dir_N(\beta \cdot \vec{1})$ that involves allocating $p_{k,c}$ proportion of data examples for class c to client k where $\vec{1}$ is the vector of ones.

CIFAR-10. CIFAR-10 [29] is the popular classification benchmark dataset. CIFAR-10 consists of 32×32 resolution images in 10 classes, with 6,000 images per class. We use 50,000 images for training and 10,000 images for testing.

CIFAR-100. CIFAR-100 [29] is the popular classification benchmark dataset. CIFAR-100 consists of 32×32 resolution images in 100 classes, with 6,000 images per class. We use 50,000 images for training and 10,000 images for testing.

PathMNIST. PathMNIST [26] is a collection of 10 pre-processed medical open datasets. It is standardizded to perform classification tasks on light weight 28×28 images, which requires no background knowledge, while we apply the image size as 32×32 . PathMNIST has 9 classes and three subsets: training, validation, and test. Each has 89,996 data whose label distribution is near balanced, but unbalanced, and we do not use the validation subset for training. Figure 8 shows several images from the training dataset.

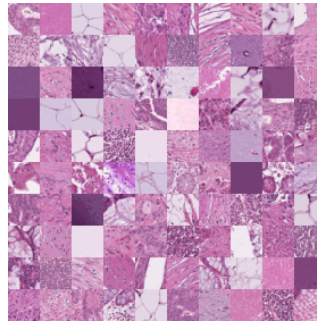


Figure 8: PathMNIST Images.

Specification. We describe the detailed specification regarding ‘Big’, ‘Medium’, ‘Small’ models. Deservedly, other medium-size models also are able to be sampled from the supernet while the trade-off between resources and accuracies happens (Figure 5).

Table 8: Specification for the child models sampled from the supernet. We report inference time in milliseconds, model size in million (M) units, and FLOPS in billions (B) units of parameters.

Child Model	Big (B)	Medium (M)	Small (S)
Inference Time	0.37 (ms)	0.20 (ms)	0.06 (ms)
Model Size	0.40 (M)	2.47 (M)	3.08 (M)
FLOPS	2.07 (B)	6.01 (B)	13.36 (B)

F Additional Experimental Results

F.1 Global Accuracies

Unlike the main section, we evaluate a global accuracy of each server model with original test dataset (Table 9, Table 10, Table 11, Table 12, Table 13, Table 14).

Table 9: Performance of FedSup on CIFAR-10 test dataset with supernet having only dynamic depth. (last accuracy / best accuracy) is written in order ($f = 0.1, N = 100$).

τ	m	Dirichlet		Shard	
		$\beta = 0.01$	$\beta = 1.0$	s=2	s=10
1	0.0	21.28 / 29.05	71.04 / 71.56	48.53 / 52.70	69.10 / 71.59
	0.1	28.96 / 32.08	70.07 / 72.41	52.57 / 55.84	72.47 / 73.24
	0.5	23.47 / 31.62	70.89 / 74.13	49.54 / 60.09	75.18 / 76.19
5	0.0	33.59 / 42.82	75.61 / 76.80	54.22 / 62.78	76.57 / 77.79
	0.1	39.59 / 42.94	75.05 / 76.02	47.26 / 61.67	77.43 / 78.35
	0.5	39.76 / 45.44	75.92 / 77.18	51.94 / 62.30	74.03 / 77.21

Table 10: Performance of FedSup on CIFAR-10 test dataset with supernet having only dynamic kernel. (last accuracy / best accuracy) is written in order ($f = 0.1, N = 100$).

τ	m	Dirichlet		Shard	
		$\beta = 0.01$	$\beta = 1.0$	s=2	s=10
1	0.0	20.57 / 31.77	76.69 / 78.88	36.84 / 55.48	77.20 / 78.84
	0.1	10.78 / 30.05	77.50 / 78.78	54.46 / 58.06	78.29 / 78.29
	0.5	18.94 / 34.25	77.83 / 79.99	42.34 / 56.48	78.26 / 80.46
5	0.0	42.79 / 48.76	80.76 / 81.57	35.77 / 62.16	82.57 / 83.06
	0.1	18.89 / 44.96	79.85 / 80.88	45.81 / 63.21	80.96 / 82.84
	0.5	29.59 / 51.12	81.52 / 82.35	48.79 / 59.92	80.00 / 82.76

Table 11: Performance of FedSup on CIFAR-10 test dataset with supernet having only dynamic width. (last accuracy / best accuracy) is written in order ($f = 0.1, N = 100$).

τ	m	Dirichlet		Shard	
		$\beta = 0.01$	$\beta = 1.0$	s=2	s=10
1	0.0	24.72 / 31.07	73.67 / 75.61	38.99 / 50.04	75.56 / 76.44
	0.1	27.30 / 33.77	74.85 / 76.34	38.95 / 54.33	75.22 / 76.04
	0.5	26.04 / 30.24	77.65 / 77.85	33.66 / 50.03	77.89 / 78.12
5	0.0	32.98 / 40.88	78.48 / 79.34	51.84 / 57.85	80.03 / 80.14
	0.1	31.39 / 42.89	78.29 / 78.49	43.28 / 56.86	78.48 / 80.10
	0.5	32.53 / 43.01	79.56 / 79.82	51.06 / 59.33	77.86 / 80.37

Table 12: Performance of E-FedSup on CIFAR-10 test dataset with supernet having only dynamic depth. (last accuracy / best accuracy) is written in order ($f = 0.1, N = 100$).

τ	m	Dirichlet		Shard	
		$\beta = 0.01$	$\beta = 1.0$	s=2	s=10
1	0.0	25.76 / 31.89	71.16 / 72.80	37.18 / 53.33	71.38 / 72.59
	0.1	25.84 / 35.11	73.17 / 73.21	42.01 / 53.11	73.13 / 73.27
	0.5	17.75 / 32.58	75.26 / 75.73	52.95 / 57.48	74.19 / 76.03
5	0.0	34.85 / 41.96	79.28 / 79.59	51.94 / 63.70	80.37 / 81.01
	0.1	28.96 / 40.77	80.19 / 80.19	60.48 / 65.21	81.41 / 81.60
	0.5	24.34 / 43.42	80.53 / 81.10	40.22 / 62.49	81.51 / 81.78

Table 13: Performance of E-FedSup on CIFAR-10 test dataset with supernet having only dynamic kernel. (last accuracy / best accuracy) is written in order ($f = 0.1, N = 100$).

τ	m	Dirichlet		Shard	
		$\beta = 0.01$	$\beta = 1.0$	s=2	s=10
1	0.0	22.08 / 31.71	75.79 / 76.97	46.71 / 54.07	74.68 / 77.30
	0.1	24.20 / 32.36	76.66 / 76.93	43.80 / 57.80	75.22 / 77.35
	0.5	26.75 / 34.95	77.94 / 78.59	32.61 / 54.86	79.28 / 79.28
5	0.0	38.27 / 42.90	79.56 / 80.75	46.11 / 60.77	81.33 / 82.54
	0.1	24.08 / 43.91	79.51 / 80.78	54.85 / 61.71	81.16 / 82.32
	0.5	31.97 / 50.82	80.74 / 81.93	21.26 / 43.72	82.01 / 82.61

Table 14: Performance of E-FedSup on CIFAR-10 test dataset with supernet having only dynamic width. (last accuracy / best accuracy) is written in order ($f = 0.1, N = 100$).

τ	m	Dirichlet		Shard	
		$\beta = 0.01$	$\beta = 1.0$	s=2	s=10
1	0.0	17.70 / 27.93	72.20 / 72.63	39.45 / 48.52	73.93 / 73.93
	0.1	20.07 / 30.38	74.64 / 74.73	36.08 / 51.81	72.99 / 74.30
	0.5	16.68 / 30.32	77.90 / 77.90	36.63 / 51.81	75.71 / 76.29
5	0.0	32.18 / 38.54	78.42 / 80.15	43.34 / 59.88	79.27 / 80.83
	0.1	23.56 / 39.97	78.35 / 78.86	37.13 / 59.98	80.81 / 80.81
	0.5	32.80 / 38.32	79.84 / 80.29	51.40 / 59.92	80.35 / 81.16

F.2 Learning Curve of Global Accuracy

We visualize the learning curves of the networks trained with FedSup and E-FedSup (Figure 9). As Figure 9 shows, FedSup has slightly better performance than E-FedSup. Here, the cosine learning rate scheduler is used, and the detailed explanations are noted in Section 4.

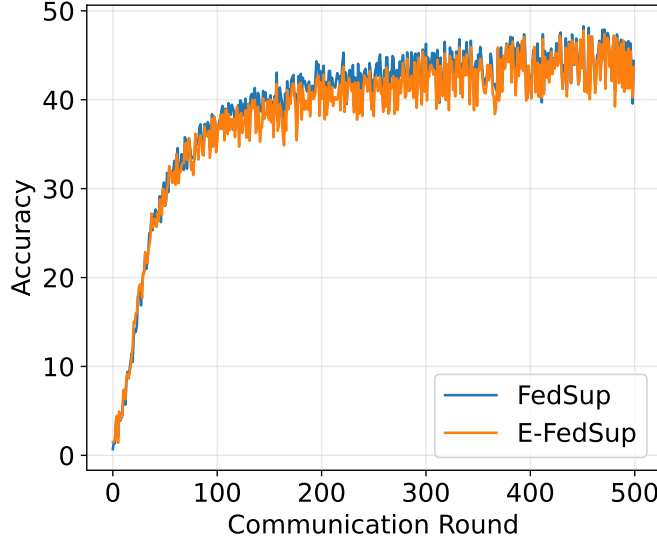


Figure 9: Learning curve of the networks trained with FedSup and E-FedSup. Both networks are trained with $s = 50$, $\tau = 5$, $f = 0.1$, $N = 100$.

F.3 PathMNIST Results

As mentioned in Table 5, FedSup and E-FedSup works better than FedAvg algorithm. Most performances in Table 15 are lower than the values in Table 15.

Table 15: FedAvg performance on PathMNIST ($N = 100$, $\tau = 5$).

f	m	$\beta = 100.0$		$\beta = 1.0$	
		Initial	Personalized	Initial	Personalized
1.0	0.0	72.21 ± 4.67	72.09 ± 4.30	69.95 ± 6.94	77.00 ± 6.26
0.1	0.0	71.15 ± 4.43	72.12 ± 4.69	67.87 ± 6.78	76.77 ± 7.34

F.4 Inplace Distillation: Representation Divergence

Table 16 describes the initial and personalized accuracy according to the inplace distillation. The inplace-distillation is not applied during the fine-tuning of personalization. In most cases, applying inplace distillation improves the performance.

Table 16: Initial and personalized accuracy of FedSup on CIFAR-100 with and without inplace distillation. The fine-tuning epochs is 5, f is 0.1, N is 100, and s is 10.

Architecture	Size	B		M		S	
		In-Distill	Initial	Personalized	Initial	Personalized	Initial
FedSup	True	34.54 ± 7.04	69.98 ± 6.89	34.40 ± 6.29	70.83 ± 6.11	33.40 ± 6.25	68.34 ± 6.89
	False	33.12 ± 7.19	68.80 ± 7.01	32.54 ± 6.75	68.73 ± 7.11	30.52 ± 7.02	67.24 ± 7.44

F.5 FedProx: Weight Divergence

Table 17 describes the initial and personalized accuracy according to the FedProx. The FedProx is not applied during the fine-tuning of personalization. In most cases, there remains little changes in performance after applying FedProx. Here, we use the value of hyperparameter λ in FedProx as 0.001.

Table 17: Initial and personalized accuracy of FedSup on CIFAR-100 with and without FedProx. The fine-tuning epochs is 5, f is 0.1, N is 100, and s is 10.

Architecture	FedProx	B		M		S	
		Initial	Personalized	Initial	Personalized	Initial	Personalized
FedSup	X	34.54 \pm 7.04	69.98 \pm 6.89	34.40 \pm 6.29	70.83 \pm 6.11	33.40 \pm 6.25	68.34 \pm 6.89
	O	34.44 \pm 6.55	69.91 \pm 6.79	34.46 \pm 6.31	70.79 \pm 6.15	33.49 \pm 6.50	68.01 \pm 6.77

F.6 Training Time Analysis on Synchronized Training Settings

Our methods are much more efficient in terms of time than the synchronous training of FedAvg-Variant methods. Consider an example for real-world applications. Since IoT, Edge Device, and Cloud Server have different resource performance, the time it takes for local training is different for each machine. We assume the local training time for every round in Table 18. If you need to train with FedAvg-Variant Model, the time it takes to synchronize every round is 30 (sec) + network bandwidth time. On the other hand, in the case of E-FedSup, the model is distributed in consideration of the resource, S for IoT, M for Edge Device, and B for Cloud Server, FL can be implemented so that 10 (sec) + network bandwidth time is required. FedSup can also be implemented much more effectively than FedAvg-variant methods if sub-models are selected well in local training.

Table 18: Assuming that the local training time of the Big model in the IoT device is 30 seconds, the training time in different machines of different models is assumed based on this.

	B	M	S
IoT	30(sec)	20(sec)	10(sec)
Edge Device	20(sec)	10(sec)	6(sec)
Cloud Server	10(sec)	5(sec)	3(sec)

F.7 Communication Cost Analysis

Figure 10 is a graph depicting the communication cost required for the neural network to reach 36% accuracy on CIFAR-100 ($N = 100$, $f = 0.1$, $s = 10$). E-FedSup is the most efficient, and FedSup has the same communication cost as FedAvg for each round, but the performance converges faster.

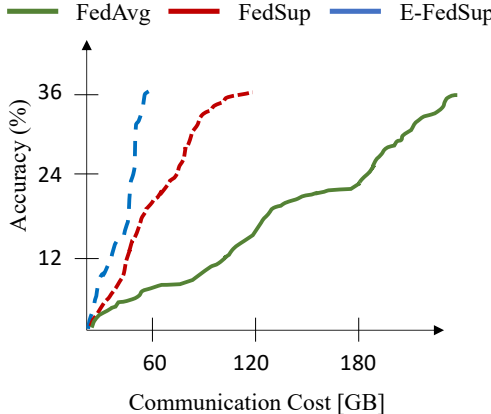


Figure 10: Comparison of communication costs with FedAvg, FedSup, and E-FedSup. The communication cost paid until reaching the same accuracy is compared.

F.8 Number of Sampled Architectures for Training in FedSup

We study the number of sampled architectures M per training iterations. It is important because larger n leads to more training time. We train the models with n equal to 1,2,3, or 4 where the sandwich rule is not applied when $n \leq 2$.

Table 19: Performance of FedSup on CIFAR-10 test dataset with supernet having dynamic operations on depth, kernel, and width. (accuracy on Dirichlet distribution having $\beta = 0.01$ / accuracy on Dirichlet distribution having $\beta = 1.0$) is written in order ($f = 0.1, N = 100, \tau = 5, m = 0.5$).

M	1	2	3	4
W/ Sandwich Rule	-	-	45.44 / 77.79	45.12 / 76.78
W/O Sandwich Rule	43.64 / 77.68	41.58 / 77.27	43.08 / 76.61	43.83 / 77.27